

1 The Wood equation allows consistent fitting of individual antibody responses profiles in  
2 Zika virus or SARS-CoV-2 infected patients

3

4 J. Denis<sup>1,2</sup>, A. Garnier<sup>1</sup>, D. Claverie<sup>3</sup>, F. De Laval<sup>4,5</sup>, S. Attoumani<sup>6</sup>, B. Tenebray<sup>2,6</sup>, G.A.  
5 Durand<sup>2,6</sup>, B. Coutard<sup>6</sup>, I. Leparc-Goffart<sup>2,6</sup>, JN. Tournier<sup>1,7,8</sup>, S. Briolant<sup>9,10</sup>, and C.  
6 Badaut<sup>1,6</sup>

7

8 1 Unité de Biothérapies anti-Infectieuses et Immunité, Institut de Recherche  
9 Biomédicale des Armées, 1 place du Général Valérie André BP73, Brétigny-sur-Orge  
10 Cedex, France.

11 2 Centre National de Référence des Arbovirus, Institut de Recherche Biomédicale des  
12 Armées, Marseille, France.

13 3 Unité de Neurophysiologie du Stress, Institut de Recherche Biomédicale des Armées, 1  
14 place du Général Valérie André BP73, Brétigny-sur-Orge Cedex, France.

15 4 Service de Santé des Armées, Centre d'Epidémiologie et de Santé Public des Armées,  
16 Marseille, France.

17 5 Aix Marseille Université, INSERM, SESSTIM, Science Economique & Sociales de la Santé  
18 & Traitement de l'Information Médicale, Marseille, France.

19 6 Unité des Virus Émergents (UVE: Aix-Marseille Univ - IRD 190 - Inserm 1207 - IHU  
20 Méditerranée Infection), Marseille, France.

21 7 Institut Pasteur, Innovative Vaccine Laboratory, Paris, France

22 8 Ecole du Val-de-Grâce, Paris, France.

23 9 Unité de Parasitologie et Entomologie, Département des Maladies Infectieuses, Institut  
24 de Recherche Biomédicale des Armées, Marseille, France.

25 10 Aix Marseille Université, IRD, AP-HM, SSA, UMR vecteurs – Infections Tropicales et  
26 Méditerranéennes (VITROME), IHU – Méditerranée Infection, Marseille, France.

27

## 28 **Abstract**

29 Antibody kinetic curves obtained during a viral infection are often fitted using  
30 aggregated data from patients, hiding the heterogeneity of patient responses. The Wood  
31 equation makes it possible to establish the link between an individual's kinetic profile  
32 and the disease, which may be helpful in identifying and studying clusters.

33

## 34 **Keywords**

35 Humoral immune response, curve fit, Zika virus, SARS-CoV-2, kinetic

## 36 **Introduction**

37 Viral infections are followed by an immune response, generally leading to increased  
38 antibody levels. The severity of the disease following infection with severe acute  
39 respiratory syndrome coronavirus 2 (SARS-CoV-2) can be related to the antibody  
40 kinetics [1]. Several studies have also shown a difference in the kinetic profiles of anti-  
41 Zika virus (ZIKV) antibodies, depending on whether or not there was a pre-dengue  
42 infection [2].

43 IgG/IgM kinetic profiles may allow investigation of the link between a humoral immune  
44 response and its involvement in the severity of the resulting disease until its  
45 disappearance or clearance of the infecting virus. The immune response is characterized  
46 by the amplitude of the antibody response and the day on which they become  
47 detectable, their concentration is maximal, and they become undetectable. These data  
48 are difficult to obtain. Furthermore, data from various patients are often incomplete and

49 aggregated to obtain an average kinetic curve that does not account for the  
50 heterogeneity of the humoral immune response of each patient. Here, we propose using  
51 Wood's equation to adjust the experimental data obtained from patient samples  
52 collected over several weeks to obtain information from each patient. Such data could  
53 allow the association of certain pathologies with the characteristics of the antibody  
54 response. The addition of such epidemiological data, combined with the use of artificial  
55 intelligence, could provide clues to the possible involvement of the humoral immune  
56 response in patient recovery. We selected two models of emerging viral infection (Zika  
57 virus and SARS-CoV-2) that have different modes of transmission and clinical  
58 manifestations for which Wood's formula perfectly describes the kinetics of the  
59 antibodies induced.

60 Wood's equation was first routinely used to follow milk production of cattle [3], a  
61 biological process of protein production. It is now commonly used to adjust the kinetics  
62 of viraemia [4] and estimate IgG concentrations after vaccination [5]. We used this  
63 equation to extrapolate unavailable constants (day when antibody detection becomes  
64 positive (pos day), day of maximal response (max day), maximal level of antibody (max  
65 level), and day when the antibody detection becomes negative (neg day)) as  
66 characteristics of the system studied.

### 67 **Patients, materials, and methods**

68 The two SARS-CoV-2-infected patients in this study have been described [6]; the  
69 patients, who had mild or moderate disease, were called P1 and P2, respectively. Data  
70 for the three ZIKV-infected patients were extracted from a previously published cohort  
71 survey [7]. The patients, with or without previous dengue infection, were identified as  
72 P3, P4, and P5, respectively. The latter three patients presented with several symptoms

73 of varying duration: a maculopapular rash (11, 3, and 14 days for P3, P4, and P5,  
74 respectively), conjunctivitis (12, 3, and 10 days, respectively), pruritis (6 and 3 days for  
75 P3 and P4 and not recorded for P5), moderate fever (1 day for both P2 and P4),  
76 headache (18 days for P3 only), purpura (P3 only), retroorbital pain (12 days for P3  
77 only), asthenia (17 and 15 days for P3 and P4, respectively), anorexia (P3 only), diarrhea  
78 (only P5 for 6 days), arthralgia (knees, ankles, elbows, and wrists for P3 for 18 days and  
79 the knees for P4 for 2 days), myalgia (2 days for P3 only), and axial back pain (10, 3, and  
80 2 days for P3, P4, and P5, respectively). The curve fit obtained with the data of each  
81 patient was used to calculate the max day and compared to the mean of the max day for  
82 the three patients combined.

83 ELISA using total inactivated ZIKV and recombinant domain III of the ZIKV envelope  
84 protein (ZEDIII) was used to determine the IgM and IgG levels, respectively [8]. Anti-  
85 SARS-CoV-2 IgG levels were determined using the receptor-binding domain (RBD) of the  
86 spike envelope glycoprotein as target [9]. Optical-density ratios (ODr) were calculated  
87 by dividing the OD obtained with the target for the same sera with the blank. The  
88 antibody levels following infection with ZIKV or a SARS-CoV-2 infection were fitted  
89 using the Wood model ( $ODr = a \cdot Day^b \cdot \exp(-c \cdot Day) + d$ ) using KaleidaGraph 4.5 software. The  
90 positive threshold of the ODr was calculated as the mean + 3×standard deviation for  
91 each studied antibody and antigenic target (IgM for ZIKV=3.00, IgG for EDIII=1.54; IgG  
92 for RBD=2.40). Max day was calculated following the formula:  $max\ day = b/c$ . The  
93 maximum IgG levels were calculated following the formula:  $max\ level = a(b/c)^b \exp(-b)$  [4].  
94 The Wood curve was plotted day by day for each condition. Both pos day and neg day  
95 were extrapolated from each curve.

## 96 **Results**

97 The antibody kinetic profile parameters are presented in Table 1. Pos day, max day, max  
98 IgG level and neg day were 0, 54, 20.5 and 377 for P1 and 2, 43, 19.3 and 251 days for  
99 P2, respectively, for SARS-CoV-2 (Fig 1A). Pos day, max day, max antibody level, and neg  
100 day for IgM and IgG were 6, 19, 5.9, and 49, and 3, 153, 5.1 and 680 days, respectively,  
101 for P3, who presented no immunological scar, and 6, 14, 3.2, 32 days for IgM and 4, 190,  
102 21.9 and 1,660 days for IgG for P4 (Fig 1B). These data for P5 were 8, 133, 2.4, and 598  
103 days for IgG. The extrapolation of the max day (170 days) and the neg day (832 days)  
104 obtained with the curve fit of the pooled data of P3, P4, and P5 (Pooled data) was  
105 different from the calculated mean of the max day (159 days) and neg day (979 days) of  
106 the three individual curves (Fig 1C). The reliability factors were high ( $r \geq 0.88$ ), except for  
107 the pooled data curve ( $r=0.56$ ) (Table 1).

## 108 **Discussion**

109 ODr values correlate with the concentrations and avidities of antibodies, reflecting their  
110 affinity constants and therefore their ability to specifically bind to their target at a  
111 determined concentration. Although ODr's are only semi-quantitative, the maximum ODr  
112 and determined positivity threshold are intrinsic values of the system and give relevant  
113 relative values.

114 Many samples were missing during the first weeks after the infection of P1 with SARS-  
115 CoV-2, but adjustment of the obtained curve gave results close to those of the adjusted  
116 curve for P2 (with a high reliability factor,  $r \geq 0.88$ ). Samples are rarely taken on pos day  
117 or max day and that for neg day is often too late to be taken, sometimes hundreds of  
118 days after the onset of symptoms. However, these missing values can be extrapolated  
119 with high reliability ( $r$  close to 1). In many studies, incomplete data from patients were

120 pooled to obtain a full fit of the kinetic curve and the characteristic constants calculated  
121 using the equation obtained by fitting the aggregate data [10 , 11].

122 The means of the max and neg days obtained from the curve fit of each patient ( $r \geq 0.91$ )  
123 were very different from the determined max and neg days obtained from a single curve  
124 fit (low  $r = 0.56$ ) of the pooled data (Figure 1C). This leads to the loss of information and  
125 the ability to observe distinct populations and, finally, to a bias in the estimation of the  
126 kinetic parameters, as the immune response varies between patients; here, according to  
127 the immune status of the scar vis-à-vis the flavivirus. We propose a method that has  
128 already been proven for other biological variables to obtain individual information  
129 rather than by pooling the data. Wood's model makes it possible to adjust the kinetics of  
130 each patient and then individually extract each constant.

131 We applied this method to the humoral immune response directed against two viruses  
132 that have different modes of transmission and clinical manifestations. This method  
133 allows patients to be linked to a past event, visible, for example, by the presence of a  
134 flavivirus immune scar. The patient who was previously infected with a flavivirus had a  
135 lower level of IgM directed against ZIKV and a higher level of IgG than the patient  
136 without a serological scar directed against a flavivirus, as observed in a previous study  
137 [12]. The patient with a serological scar to flavivirus showed much less symptoms than  
138 the patient without such a scar. During SARS-CoV-2 infection, the negativation of IgG  
139 directed against the RBD domain occurred faster for patient P2, who had more serious  
140 symptoms than patient P1, who had a mild form of the disease.

141 The identification of different kinetic profiles for patients would make it possible to  
142 relate a typical profile to the seriousness of the clinical signs and could be useful in  
143 predicting the intensity or evolution of the pathology and perhaps even in

144 demonstrating, a posteriori, the association of a type of humoral immune response to  
145 improvement or worsening of the patient's condition. Second, such identification could  
146 contribute to the exploration of the mechanisms involved in severe forms and propose  
147 solutions for treating patients identified to have a similar kinetic profile. The diagnostic  
148 window could also be determined and would be useful for the diagnosis of diseases such  
149 as dengue-like syndrome or Covid-19.

150 In conclusion, we present a methodology that makes it possible to obtain otherwise  
151 unavailable individual data. These data could help identify patients with identical  
152 profiles and thus be useful in classifying immune responses associated with disease  
153 severity, highlighting mechanisms that are hidden in pooled data.

154

## 155 **Acknowledgements**

156 This work was partially supported by the European Union's Horizon H2020 Project  
157 "Advanced Nanosensing platforms for Point of care global diagnostics and surveillance"  
158 (CONVAT) (No101003544) and partially funded by the Direction Générale de  
159 l'Armement and the Service de Santé des Armées (Biomedef PDH-2-NRBC-2-B-2111),  
160 and the Direction centrale du Service de santé des armées (grant IDs: 2016RC10).

161

## 162 **Legend**

163 Figure 1

164 Antibody kinetics. **(A)** IgG of two SARS-CoV-2-infected patients, P1 (blue) and P2 (red)  
165 and **(B)** IgM (square) and IgG (circle) of ZIKV-infected patients P3 (orange) and P4  
166 (green) were fitted using the Wood equation. **(C)** The data from three patients were  
167 plotted and the curve fit performed using the Wood equation for each patient (P3:

168 orange, P4: green, P5: grey). The black curve is the fitted curve using pooled data of the  
169 three patients P1, P2, and P3. The IgM curve reliability factors  $r$  are 0.97 and 0.96 for P3  
170 and P4, respectively, and those of the IgG curve 0.93, 0.88, 0.99, 0.92, 0.91, and 0.56 for  
171 P1, P2, P3, P4, P5 and the black curve, respectively. The means and standard deviations  
172 of the optical density ratios are presented panel A.

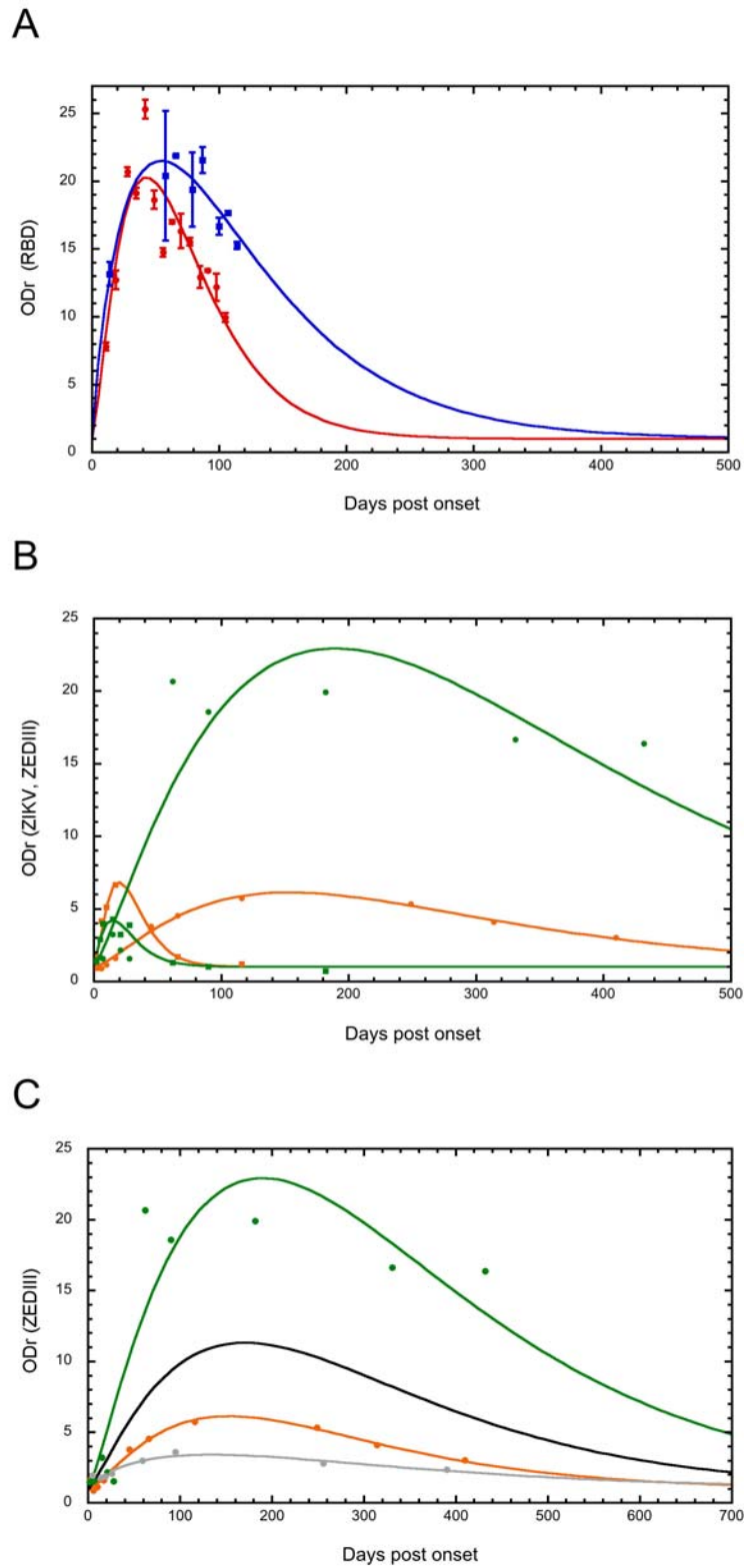


Table 1

Patient	Age	Sex	Imm. scar	Antibody type	ELISA target	a	b	c	d	r	Pos day	Max day	Max level	Neg day
P1	25-30	F	ND	IgG	RBD SARS-CoV-2	1.513	0.87006	0.015995	1	0.93	0	54	20.5	377
P2	50-55	M	ND	IgG	RBD SARS-CoV-2	0.33971	1.4658	0.034283	1	0.88	2	43	19.3	251
P3	35-40	M	No	IgM	ZIKV	0.1585	1.8327	0.094116	1	0.97	6	19	5.9	49
P3	35-40	M	No	IgG	ZEDIII	0.017577	1.4083	0.0092013	1	0.99	3	153	5.1	680
P4	40-45	M	Yes	IgM	ZIKV	0.39849	1.2568	0.08709	1	0.96	6	14	3.2	32
P4	40-45	M	Yes	IgG	ZEDIII	0.10658	1.2549	0.006617	1	0.92	4	190	21.9	1660
P5	40-45	M	ND	IgG	ZEDIII	0.12655	0.7574	0.005674	1	0.91	8	133	2.4	598
Pooled data	None	None	None	IgG	None	0.0505062	1.2854	0.0075445	1	0.56	4	170	10.3	832

Abbreviations: Imm. scar: immunological scar. a, b, c, d: Wood's constants. r: reliability factor. Pos day: day when antibody detection becomes positive. Max day: day of maximal response. Max level: maximal level of antibody. Neg day: day when the antibody detection becomes negative. ND: Not Documented. F: Female. M: Male. RBD SARS-CoV-2: receptor-binding domain of severe acute respiratory syndrome coronavirus 2. ZIKV: Zika virus. ZEDIII: recombinant domain III of the ZIKV envelope protein.

Figure 1



## References

- [1] Okba NMA, Müller MA, Li W, Wang C, GeurtsvanKessel CH, Corman VM, et al. Severe Acute Respiratory Syndrome Coronavirus 2-Specific Antibody Responses in Coronavirus Disease Patients. *Emerging infectious diseases*. 2020;26:1478-88.
- [2] Barzon L, Percivalle E, Pacenti M, Rovida F, Zavattoni M, Del Bravo P, et al. Virus and Antibody Dynamics in Travelers With Acute Zika Virus Infection. *Clinical infectious diseases : an official publication of the Infectious Diseases Society of America*. 2018;66:1173-80.
- [3] Wood PDP. Algebraic Model of the Lactation Curve in Cattle. 1967;216:164-5.
- [4] Islam ZU, Bishop SC, Savill NJ, Rowland RR, Lunney JK, Tribble B, et al. Quantitative analysis of porcine reproductive and respiratory syndrome (PRRS) viremia profiles from experimental infection: a statistical modelling approach. *PLoS One*. 2013;8:e83567.
- [5] Andraud M, Fablet C, Renson P, Eono F, Mahé S, Bourry O, et al. Estimating Parameters Related to the Lifespan of Passively Transferred and Vaccine-Induced Porcine Reproductive and Respiratory Syndrome Virus Type I Antibodies by Modeling Field Data. *Frontiers in veterinary science*. 2018;5:9.
- [6] E. Billon-Denis AF-R, A. Garnier, L. Cheutin, C. Vigne, E. Tessier<sup>1</sup>, J. Denis, C. Badaut, C. Rougeaux, F. Iseni, A. Depeille-Wuille, H. Timera, L. Boutin, G. Frenois-Veyrat, I. Drouet, N. Verguet, F. Nolent, O. Gorgé, O. Ferraris<sup>1</sup>, J.-N. Tournier. Differential serological and neutralizing antibody dynamics after an infection by a single SARS-CoV-2 strain highlights important host factors for COVID-19 immunity. in press.
- [7] de Laval F, d'Aubigny H, Matheus S, Labrousse T, Ensargueix AL, Lorenzi EM, et al. Evolution of symptoms and quality of life during Zika virus infection: A 1-year

prospective cohort study. *Journal of clinical virology : the official publication of the Pan American Society for Clinical Virology*. 2018;109:57-62.

[8] Denis J, Attoumani S, Gravier P, Tenebray B, Garnier A, Briolant S, et al. High specificity and sensitivity of Zika EDIII-based ELISA diagnosis highlighted by a large human reference panel. *PLoS neglected tropical diseases*. 2019;13:e0007747.

[9] Stadlbauer D, Amanat F, Chromikova V, Jiang K, Strohmeier S, Arunkumar GA, et al. SARS-CoV-2 Seroconversion in Humans: A Detailed Protocol for a Serological Assay, Antigen Production, and Test Setup. *Curr Protoc Microbiol*. 2020;57:e100.

[10] Padoan A, Sciacovelli L, Basso D, Negrini D, Zuin S, Cosma C, et al. IgA-Ab response to spike glycoprotein of SARS-CoV-2 in patients with COVID-19: A longitudinal study. *Clinica chimica acta; international journal of clinical chemistry*. 2020;507:164-6.

[11] Bozza FA, Moreira-Soto A, Rockstroh A, Fischer C, Nascimento AD, Calheiros AS, et al. Differential Shedding and Antibody Kinetics of Zika and Chikungunya Viruses, Brazil. *Emerging infectious diseases*. 2019;25:311-5.

[12] Cucunawangsih, Lugito NP, Kurniawan A. Immunoglobulin G (IgG) to IgM ratio in secondary adult dengue infection using samples from early days of symptoms onset. *BMC infectious diseases*. 2015;15:276.